Luminescent Carbon Nanotubes for Biomedical Diagnosis and Treatment

Y. Guo[*], W. Wang[*], H. S. Cho[*], J. Lian[**], R. Ewing[**], L. Wang[**], G. K. Liu[***], Z.Y. Dong[****] and D. Shi[*]

[*] Dept. of Chemical and Materials Engineering, University of Cincinnati, Cincinnati, Ohio 45221, shid@email.uc.edu

[**] Dept. of Geological Sciences, Nuclear Engineering & Radiological Sciences and Materials Science & Engineering, University of Michigan, Ann Arbor, Michigan 48109

[***] Chemistry Division, Argonne National Laboratory, Argonne, Illinois 60439

[****] Dept. of Internal Medicine, College of Medicine, University of Cincinnati, Cincinnati, OH 45221

ABSTRACT

In the diagnosis and treatment of cancer, nanoparticles not only need a "cavity" structure for storage and delivery of drugs, but also must be luminescent in order to track and diagnose effectiveness of the treatment. Here, we present a novel method for the deposition of nano-sized, europium doped Y_2O_3 phosphors onto the surfaces of multi-walled carbon nanotubes (MWCNTs). The surface morphologies and microstructure have been characterized by high resolution transmission electron microscopy (HRTEM). Fluorescent spectrometer measurements confirm that the surface-functionalized MWCNTs exhibit luminescence in the visible light range. The deposition of optically-activated rare-earth nanoparticles on the surface of carbon nanotubes may find important applications in cancer diagnosis and treatment. The nucleation and growth mechanisms of rare-earth doped nano-phosphors on MWCNTs are described and discussed.

Keywords: rare earth, luminescent, carbon nanotube, surface morphologies, nucleation and growth mechanisms.

1 INTRODUCTION TO SURFACE FUNCTIONALIZATION FOR CANCER DIAGNOSIS NANOTECHNOLOGY

There has been an increasing need for the application of nanotechnology in the area of cancer diagnosis and therapy. Nanoparticles and nanotubes, by novel design at nanometer scale, can be used as drug vehicles that can target tumor tissues or cells. Nanoparticles and nanotubes can also be functionalized for qualitative or quantitative detection of tumor cells. However, in both cancer diagnosis and treatment, specific mechanisms of biomarking and drug delivery have to be identified, based on which novel nanostructures maybe developed for these goals.

Anticancer drug delivery may require a nanoparticle to be designed as a nanosphere and a nanocapsule. The former has a low density network structure in which the drug is dispersed throughout the particle, while the latter possesses a vesicular system in which the drug is confined to a cavity surrounded by a single layer membrane [1]. In such a design, not only has the drug be delivered to a specific cell region, but also protected from premature inactivation during its transport. The previous work has shown that the accumulation of intravenously injected nanoparticles relies on a passive diffusion or convection across the leaky, hyperpermeable tumor vasculature [2]. The drug uptake can also be influenced by the ligand decorated nanoparticles [3].

Surface functionalization of carbon nanotubes is an effective way of improving the solubility and dispersion of the nanotubes in aqueous solutions and to design new hybrid materials by coupling the properties of novel nanostructures to the carbon nanotubes. [4–7] Functionalization of carbon nanotubes can be achieved either by covalent or non-covalent methodologies. [8–12] The attachment of metal nanoparticles, particularly Au nanoparticles, to functionalized carbon nanotubes has recently been an active field of research for gas-sensor and catalytic applications. [13–17] In addition, various biological applications of the functionalized carbon nanotubes have been proposed, such as DNA [18] and protein biosensors, [11,19] biocatalysts, and bioseparators. [20]

2 LUMINESCENT CARBON NANOTUBES BY SURFACE FUNCTIONALIZATION

In this paper, we present experimental data on the surface deposition of rare earth doped Y_2O_3 on multi-wall carbon nanotubes (MWCNTs). The surface structures of coated MWCNTs are studied by high resolution transmission microscopy. Laser spectroscopic experiments have been carried out to study the optical behaviors of functionalized MWCNTs.

Commercial grade Pyrograf III MWCNTs were used as substrates [21]. These MWCNTs were 70-200 nm in diameter and several microns in length as can be seen in Figure 2. The rare-earth doped Y_2O_3 was deposited on MWCNTs by a solution method developed in our laboratory [22]. The starting materials of carbon nanotubes were dispersed in 250 ml distilled water by ultrasonic vibration for 0.5 h and allowed for 1h stabilization. Certain volumes of the solutions containing europium and yttrium

were added into the colloid respectively and vibrated for 0.5 h. Aqueous ammonia was dropped into the solution, allowing for at least 10 h incubation. The solution was heated at 80 °C to entirely evaporate the water. The temperature of the drying process was strictly controlled and the heating rate varied over different temperature ranges. The powder was separated from the suspension by centrifugation, rinsed several times to remove adsorbed ammonia and chloride ions, dried in air and ground. The dried powder was subsequently heat treated at 650 ºC and 950 ºC for 12h, respectively.

The functionalized MWCNT surface structure and morphology were studied by using a JEOL 2010F transmission electron microscope. The TEM samples of MWCNTs were prepared by dispersing them directly on perforated carbon films supported with Cu grids. Laser spectroscopic experiments were completed in order to study the optical behavior of the functionalized MWCNTs.

Figure 1 shows the TEM images of surface functionalized MWCNTs there were heat treated at 650 ºC. As can be seen in Fig. 1(a), the outer surface of the nanotube is quite uniformly coated by a thin film of 10 nm. A further investigation of TEM on the nanotube surface has shown crystallization of the coating thin film as shown in Fig. 1 (b), the high resolution TEM images clearly show the crystalline features of coating film on the nanotube surface from two different regions.

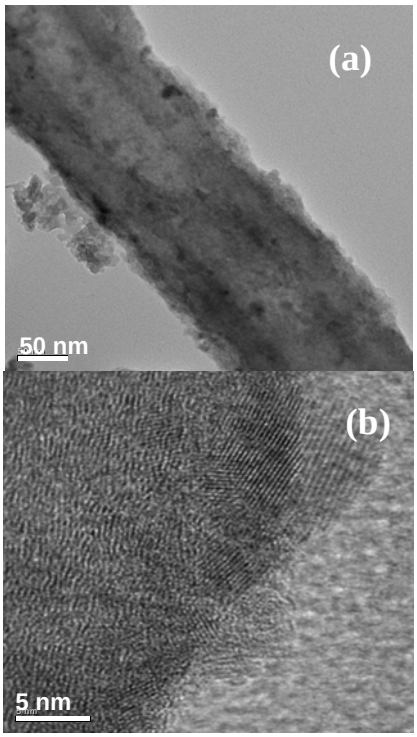

Figure 1: (a) TEM showing the surface deposition and (b) High resolution TEM showing crystalline feature of Eu-doped Y_2O_3 film on a MWCNT, heat treated at 650 ºC.

The surface coating morphology exhibits a drastic change as the heat treatment temperature is raised from 650 ºC to 950 ºC, as shown in Figure 2. The surface coating appears to be transformed from a uniform thin film (Fig. 1) to quite well dispersed nano size nuclei. At a considerably higher temperature of 950 ºC, the deposited Eu-doped Y_2O_3 particles tend to spheroidized in order to further minimize their surface energies. As can be seen in Figure 2, these spheroidites are fine crystallites with an average diameter of 5 nm. Due to relatively high energies in the initial stage of nucleation and growth, these fine crystallites are not energetically stable. At elevated temperatures, they will continue to grow. The growth of these fine crystallites requires mass transport towards them. Therefore, each crystallite may grow in the expense of the surface thin film, leading to separated, dispersed, and larger (10–20 nm) nanoparticles of Eu-doped Y_2O_3.

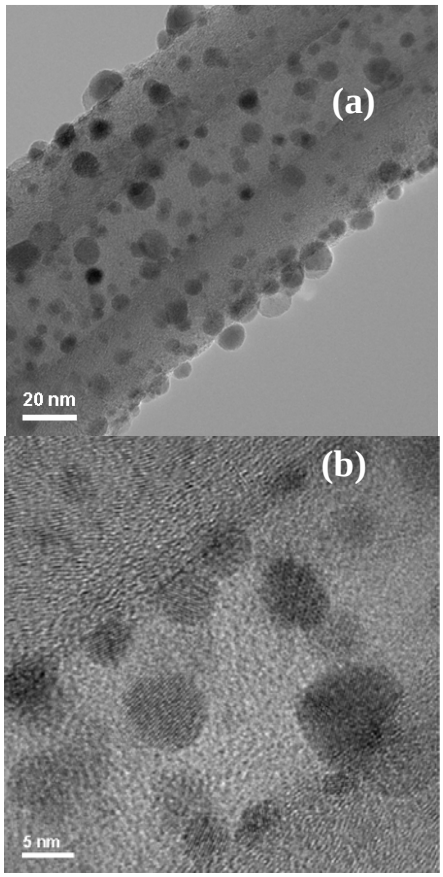

Figure 2: (a) TEM image showing the surface deposition of Er_2O_3 on a WMCNT, heat treated at 950 ºC. (b) High resolution TEM image showing the Er_2O_3 nanoparticles absorbed at the hollow core of MWCNT.

NSTI-Nanotech 2007, www.nsti.org, ISBN 1420061836 Vol. 2, 2007

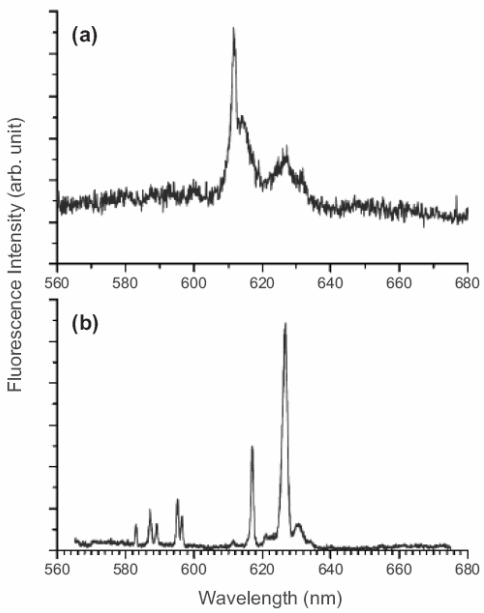

Figure 3: Luminescence emission spectra of Eu_2O_3 coated MWCNT (a) heat treated at 650 ºC and (b) at 950 ºC.

Under a 355-nm pulsed laser excitation, Eu^{3+} luminescence was observed at room temperature from samples of the coated MWCNTs heat-treated at 650 ºC and 950 ºC (Fig. 3). As shown in Fig. 3(a) and (b), the emission lines characterize the Eu^{3+} 5D0 – 7FJ (J=0,1,2) electronic transitions. In comparison, the efficiency of luminescence emission from the sample treated at 950 ºC is much higher than that from the sample treated at 650 ºC. The sharp lines in the emission spectrum of the sample treated at 950 ºC indicate that Eu^{3+} doped in Y_2O_3 has well defined crystalline structure, whereas the broader spectrum of the sample treated at 650 ºC suggests a more disordered lattice structure.

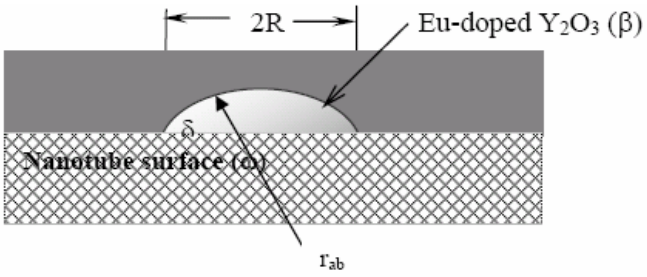

Figure 4: Schematic diagram showing the dihedral angle between the Eu-doped Y_2O_3 particle and the surface of MWCNTs.

To understand the nucleation of Eu-doped Y_2O_3 particles on the MWCNT, we may consider the surface defects on the nanotubes. From the TEM observations, these MWCNTs have a high density of surface defects which can serve as nucleation sites. Assuming that the Eu-doped Y_2O_3 particle initially forms as a spherical cap on the nanotube surface (see Fig. 4), that is, the Eu-doped Y_2O_3 is a portion of the sphere having radius r_{ab}. As viewed from above (Fig. 4 is a side view), the Eu-doped Y_2O_3 particle is a circle with a radius, R. The change in surface energy produced by formation of the Eu-doped Y_2O_3 particle on the surface of nanotube can be deduced from considering that the surface free energy is equal to the surface tension:

$$\Delta G = [A_{\alpha\beta}\gamma_{\alpha\beta} + A_{\beta\omega}\gamma_{\beta\omega}] - A_{\beta\omega}\gamma_{\alpha\omega}, \quad (1)$$

Where $A_{\alpha\omega}$ is the area of the α–β interface, $A_{\beta\omega}$ is the area of the β–ω interface, and γ is the surface tension. Here β is Eu-doped Y_2O_3 and ω is carbon nanotube. Notice that the surface energy of the α–ω interface that was eliminated when the Eu-doped Y_2O_3 phase formed, and the area of this lost α–ω interface is exactly $A_{\beta\omega}$. δ is the so-called dihedral angle.

Using the classic heterogeneous nucleation theory, the expression for the total free energy change upon forming the spherical cap nucleus is given as:

$$\Delta G = \Delta G\,(\text{bulk}) + \Delta G\,(\text{surface}) = V_\beta \Delta G_\beta + (A_{\alpha\beta} - \pi R^2 S)\gamma_{\alpha\beta}, \quad (2)$$

where $S = \cos\delta$ and $A_{\beta\omega} = \pi R^2$. This equation can be further written as

$$\Delta G = \pi r 3_{\alpha\beta}[(2-3S+S3)/3]\,\Delta G + [2\pi r^2_{\alpha\beta}(1-S) - \pi r^2_{\alpha\beta}(\sin^2\delta)S]r_{\alpha\beta} \quad (3)$$

If we recognize:

$$V_\beta = \pi r^3_{\alpha\beta}[(2-3S+S3)/3],\ A_{\alpha\beta} = 2\pi r^2_{\alpha\beta}[1-S],\ R = r_{\alpha\beta}\sin\delta,\ \sin^2\delta = 1-S \quad (4)$$

Then,

$$\Delta G = [(4/3)\, r^3_{\alpha\beta}\Delta G_\beta + 4\pi r^2_{\alpha\beta}\gamma_{\alpha\beta}][(2-3S+S3)/4] \quad (5)$$

Comparing Eq. (5) to the free energy term in the homogeneous nucleation, we obtain:

$$G\,(\text{on a surface}) = G^*(\text{not on a surface})\,[(2-3S+S3)/4] \quad (6)$$

The term in the brackets varies from 0 to 1 as the dihedral angle δ varies from 0º to 180º. The critical radius of the cap can be expressed as:

$$R^* = (2\gamma_{\alpha\beta}/\Delta G_\beta)\sin\delta = r^*_{\alpha\beta}\sin\delta \quad (7)$$

As δ increases, the value of R* decreases, the volume of the Eu-doped Y_2O_3 sphere on the nanotube surface will become smaller and, hence require fewer atoms for its formation. At δ = 0 the volume becomes zero, so that one expects the highest wetability of the Eu-doped Y_2O_3 particle on the nanotube surface.

On deposition of Eu-doped Y_2O_3, one desires that the Eu-doped Y_2O_3 particle wet the nanotube surface with minimum thermal energy. Consequently, according to above model, one requires that the Eu-doped Y_2O_3 particle have a small dihedral angle δ with the MWCNT surface. This requires a small value of $\gamma_{CNT\text{-}Y2O3}$. Interfaces with small γ are characterized by a good atomic-scale structural match at the interface. Both Y_2O_3 and MWCNT have hexagonal structures, and this will contribute to the reduction in δ and γ. Therefore, it is energetically much easier for the small Y_2O_3 particles to nucleate and grow on the MWCNT surface and form a uniform film at the low temperature of 650 ºC (Fig. 1). At a considerably higher temperature of 950 ºC, the deposited Eu-doped Y_2O_3 particles tend to become more spherical in order to further minimize their surface energies. As can be seen in Fig. 1, these nanoparticles are fine crystallites with an average diameter of ~5 nm at 650 ºC. Due to relatively high energies in the initial stage of nucleation and growth, these fine crystallites are not energetically stable. At elevated temperatures (Fig. 2), they will continue to grow. The growth of these fine crystallites requires mass transport towards them. Therefore, each crystallite may grow at the expense of the surface thin film, leading to separated, dispersed, and larger (10~20 nm) nanoparticles of Eu-doped Y_2O_3.

3 CONCLUSIONS

In summary, based on a novel design, rare-earth doped Y_2O_3 has been deposited onto the outside surfaces of the MWCNTs for the purpose of cancer diagnosis and drug delivery. Due to the small dihedral angle of Y_2O_3, the deposited Y_2O_3 exhibits a small-angle lattice interface with the nanotube substrate. The rare-earth doped Y_2O_3 on MWCNT exhibits luminescent emission in the visible light range, which can be used as a biomarker for biomedical applications. The microstructure of rare-earth nanophosphors-MWCNTs composites and optical properties are tunable by controlling the annealing temperature and hence the particle size. These results suggest that one may design and fabricate optically-active rare-earth nanoparticles on the surfaces of carbon nanotubes, and these materials may find important applications for the cancer diagnosis and treatment.

ACKNOWLEDGMENTS

The TEM and SEM analyses were conducted at the Electron Microbeam Analysis Laboratory at the University of Michigan, and supported by the Office of Basic Energy Sciences of the U.S. Department of Energy under grant No. DE-FG02-97ER45656.

REFERENCES

[1] M. Ferrari, *Nature Reviews*, 5, 161, 2005.
[2] F. Yuan, *Semin. Radiat. Oncol.*, 8, 164, 1998.
[3] S.M. Moghimi, A.C. Hunter and J.C. Murray, *Pharmacol. Rev.*, 53, 283, 2001.
[4] S. S. Wong, E. Joselevich, A. T. Woolley, C. L. Cheung, C. M. Lieber, *Nature*, *394*, 52, 1998.
[5] A. Hirsch, *Angew. Chem. Int. Ed.*, *41*, 1853, 2002.
[6] D. Shi, J. Lian, P. He, L. M. Wang, W. J. Van Ooij, M. Schulz, Y. J. Liu, D. B. Mast, *Appl. Phys. Lett.*, *81*, 5216, 2002.
[7] D. Shi, J. Lian, P. He, L. M. Wang, M. Schultz, D. B. Mast, *Appl. Phys. Lett.*, *83*, 5301, 2003.
[8] M. Zheng, A. Jagota, E. D. Semke, B. A. Diner, R. S. Mclean, S. R. Lustig, R. E. Richardson, N. G. Tassi, *Nat. Mater.*, *2*, 338, 2003.
[9] A. Star, D. Steuerman, J. R. Heath, J. F. Stoddart, *Angew. Chem. Int. Ed.*, *41*, 2508, 2002.
[10] C. Richard, F. Balavoine, P. Schultz, T. W. Ebbesen, C. Mioskowski, *Science*, *300*, 775, 2003.
[11] R. J. Chen, S. Bangsaruntip, K. A. Drouvalakis, N. W. S. Kam, M. Shim, Y. Li, W. Kim, P. J. Utz, H. J. Dai, *Proc. Natl. Acad. Sci. USA*, *100*, 4984, 2003.
[12] R. J. Chen, Y. Zhang, D. Wang, H. J. Dai, *J. Am. Chem. Soc.*, *123*, 3838, 2001.
[13] B. C. Satishkumar, E. M. Vogl, A. Govindaraj, C. N. R. Rao, *J. Phys. D*, *29*, 3173, 1996.
[14] K. Jiang, A. Eitan, L. S. Schadler, P. M. Ajayan, R. W. Siegel, N. Grobert, M. Mayne, M. Reyes-Reyes, H. Terrones, M. Terrones, *Nano Lett.*, *3*, 275, 2003.
[15] A. V. Ellis, K. Vijayamohanan, R. Goswami, N. Chakrapani, L. S. Ramanathan, P. M. Ajayan, G. Ramanath, *Nano Lett.*, *3*, 279, 2003.
[16] L. Jiang, L. Gao, *Carbon*, *41*, 2923, 2003.
[17] A. Fasi, I. Palinko, J. W. Seo, Z. Konya, K. Hernadi, I. Kiricsi, *Chem. Phys. Lett.*, *372*, 848, 2003.
[18] K. A. Williams, P. T. Veenhuizen, B. G. de la Torre, R. Eritja, C. Dekker, *Nature*, *420*, 761, 2002.
[19] J. J. Gooding, R. Wibowo, J. Q. Liu,W. R. Yang, D. Losic, S. Orbons, F. J. Mearns, J. G. Shapter, D. B. Hibbert, *J. Am. Chem. Soc.*, *125*, 9006, 2003.
[20] D. T. Mitchell, S. B. Lee, L. Trofin, N. Li, T. K. Nevanen, H. Soderlund, C. R. Martin, *J. Am. Chem. Soc.*, *124*, 11 864, 2002.
[21] Applied Sciences Inc., www.apsci.com.
[22] X. Y. Chen, L. Yang, R. E. Cook, S. Skanthakumar, D. Shi, G. K. Liu, *NanoTechnology*, 14, 670, 2003.